0026-895X/08/7302-369–378$20.00
MOLECULAR PHARMACOLOGY
Copyright © 2008 The American Society for Pharmacology and Experimental Therapeutics
Mol Pharmacol 73:369–378, 2008

Vol. 73, No. 2
40733/3297306
Printed in U.S.A.

The β1 Subunit of L-Type Voltage-Gated Ca^{2+} Channels Independently Binds to and Inhibits the Gating of Large-Conductance Ca^{2+}-Activated K^+ Channels

Shengwei Zou, Smita Jha, Eun Young Kim, and Stuart E. Dryer

Department of Biology and Biochemistry, University of Houston, Houston, Texas

Received August 8, 2007; accepted November 7, 2007

ABSTRACT

Large-conductance Ca^{2+}-activated K^+ (BK_{Ca}) channels encoded by the *Slo1* gene are ubiquitously expressed, and they play a role in regulation of many cell types. In excitable cells, BK_{Ca} channels and voltage-activated Ca^{2+} channels often form functional complexes that allow the cytoplasmic domains of BK_{Ca} channels to lie within spatially discrete calcium microdomains. Here, we report a novel protein interaction between the β1-subunit of L-type voltage-activated calcium channels ($Ca_v\beta1$) and critical regulatory domains of Slo1 that can occur in the absence of other proteins. This interaction was identified by a yeast two-hybrid screen, and it was confirmed by confocal microscopy in native neurons, by coimmunoprecipitation, and by direct binding assays. The $Ca_v\beta1$ subunit binds within the calcium bowl domain of Slo1 that mediates a portion of high-affinity Ca^{2+} binding to BK_{Ca} channels and also to a noncanonical Src homology 3 (SH3) domain-binding motif within Slo1. Binding of $Ca_v\beta1$ markedly slows Slo1 activation kinetics, and it causes a significant decrease in Ca^{2+} sensitivity in inside-out and in dialyzed cells, even in the absence of pore-forming subunits of voltage-gated Ca^{2+} channels. The guanylate kinase domain of $Ca_v\beta1$ mediates Slo1 regulation through its binding to calcium bowl domains, and this domain of $Ca_v\beta1$ is necessary and sufficient for the observed effects on BK_{Ca} activation. Binding of $Ca_v\beta1$ to SH3-binding motifs may stabilize the interaction with Slo1, or it may contribute to formation of other complexes, but it does not seem to affect Ca^{2+}-dependent gating of Slo1. Binding of $Ca_v\beta1$ does not affect cell surface expression of Slo1 in human embryonic kidney 293T cells.

Large-conductance Ca^{2+}-activated K^+ (BK_{Ca}) channels are expressed in excitable and nonexcitable tissues, including neurons, myocytes, secretory cells, and epithelial cells. These channels are cooperatively activated by membrane depolarization and binding of cytosolic Ca^{2+}, which in the presence of other channels contributes to regulation of waveform and frequency of action potential discharge, initiation and spread of dendritic Ca^{2+} spikes, control of membrane potential oscillations, release of hormones and neurotransmitters, and modulation of muscle contraction (Salkoff et al., 2006).

The pore-forming subunits of BK_{Ca} channels are encoded by the *Slo1* gene (also known as *KCNMA1*), and they contain a core region with seven membrane-spanning domains. In addition, Slo1 proteins have an unusually large cytoplasmic tail that is subjected to extensive alternative splicing, yielding channel variants with markedly different voltage and Ca^{2+} sensitivities (Shipston, 2001). The allosteric relationship between membrane potential and cytosolic Ca^{2+} in the control of BK_{Ca} gating has been studied extensively (Magleby, 2003). Voltage regulation of channel gating is associated with domains in the core regions of BK_{Ca} channels (Díaz et al., 1998), whereas the regulator of conductance of K^+ (Jiang et al., 2001; Xia et al., 2002) and calcium bowl domains (Schreiber and Salkoff, 1997; Bao et al., 2002; Zeng et al., 2005) in the cytoplasmic tail account for most of the Ca^{2+} regulation, although additional low-affinity Ca^{2+} binding sites may also modulate Ca^{2+} sensitivity (Zhang et al., 2001; Xia et al., 2002; Bao et al., 2004).

Although some BK_{Ca} channels can respond over a broad range of free Ca^{2+} concentrations (Thurm et al., 2005), most variants typically require micromolar concentrations for robust activation. For this reason, Slo1 channels must be close to a significant source of Ca^{2+} for the necessary Ca^{2+} con-

This study was supported by National Institutes of Health grant NS32748.
S.Z. and S.J. contributed equally to this research.
Article, publication date, and citation information can be found at http://molpharm.aspetjournals.org.
doi:10.1124/mol.107.040733.

ABBREVIATIONS: BK_{Ca}, large-conductance Ca^{2+}-activated K^+; $Ca_v\beta1$, $\beta1$ subunit of voltage-activated Ca^{2+}; Slo1, pore-forming subunit of BK_{Ca} channel; Ca_v, voltage-gated Ca^{2+}; SH3, Src homology 3; GK guanylate kinase; HA, hemagglutinin; FITC, fluorescein isothiocyanate; E9, embryonic day 9; CG, ciliary ganglion; GST glutathione transferase; PBST, phosphate-buffered saline containing 0.2% Triton X-100; HEK, human embryonic kidney; PBS, phosphate-buffered saline; RFP, red fluorescent protein; ANOVA, analysis of variance.

centrations to occur in space and time. In most excitable cells, the usual sources are voltage-gated Ca^{2+} (Ca_v) channels. Indirect evidence for the presence of BK_{Ca} channels within Ca_v-dependent "calcium microdomains" was documented several years ago (Wisgirda and Dryer 1994; Gola and Crest, 1993; Marrion and Tavalin, 1998), and these types of observations have been quantitatively refined in recent years (Prakriya and Lingle, 2000). A more recent study directly demonstrated the existence of macromolecular complexes between Slo1 and $Ca_v1.2$ (L-type), $Ca_v2.1$ (P/Q-type), and $Ca_v2.2$ (N-type) subunits in rat brain and in heterologous expression systems (Berkefeld et al., 2006).

In parasympathetic neurons of the chick ciliary ganglion, BK_{Ca} channels are functionally coupled to dihydropyridine-sensitive L-type Ca_v channels (Wisgirda and Dryer, 1994). L-type Ca^{2+} channels are made up of a single pore-forming subunit ($Ca_v1.1$ or $Ca_v1.2$), often in a complex with β-subunits ($Ca_v\beta$), which regulate the gating properties and trafficking of the resulting channels (De Waard et al., 1994; Brice et al., 1997; Dolphin, 2003). The net effect of $Ca_v\beta$ subunits is to increase L-type current and the resulting voltage-evoked Ca^{2+} influx in cells where they are expressed. The $Ca_v\beta$ subunits are members of the membrane-associated guanylate kinase family of proteins. They have a Src homology 3 (SH3) domain linked by a flexible loop to a guanylate kinase (GK)-like domain (Chen et al., 2004; Van Petegem et al., 2004). Their interaction with $Ca_v1.1$ is reversible (Bichet et al., 2000), and the GK domain of $Ca_v\beta$ is free to interact with other proteins (Chen et al., 2004; Van Petegem et al., 2004; Hidalgo et al., 2006).

In the present study, we show that an L-type Ca_v channel β-subunit ($Ca_v\beta1$), physically associates with Slo1 subunits of BK_{Ca} channels at two distinct regions: a noncanonical SH3 domain-binding motif, previously shown to link BK_{Ca} channels to the actin cytoskeleton via the adaptor protein cortactin (Tian et al., 2006), and also at sites within the calcium bowl region of Slo1. We were surprised to find that the $Ca_v\beta1$-Slo1 interaction does not require the presence of other channel subunits or any other proteins. Moreover, the interaction is functionally significant, because it markedly slows BK_{Ca} activation and deactivation kinetics and it causes a significant decrease in Ca^{2+} sensitivity that can be readily detected in both inside-out excised patch and whole-cell recordings. Finally, we show that the effects of $Ca_v\beta1$ on BK_{Ca} gating can be attributed to the interaction with the calcium bowl region of Slo1.

Materials and Methods

Plasmids and Antibodies. An expression plasmid (pCMV-Myc-Slo1) encoding N-terminal (ectofacial) Myc-tagged mouse Slo1 was provided by Dr. Min Li (Johns Hopkins University, Baltimore, MD). A plasmid encoding full-length human $Ca_v\beta1$ (accession no. NM_000723.3) was obtained from Origene (Rockville, MD). Other plasmids, including pGBKT7-$Slo1_{G785\text{-}A985}$, pDsRed-$Ca_v\beta1$, pCMV-HA-$Ca_v\beta1$, pGEXKG-$Slo1_{G785\text{-}A985}$, pGEXKG-$Slo1_{G785\text{-}L843}$, pGEXKG-$Slo1_{Q844\text{-}I883}$, pGEXKG-$Slo1_{T884\text{-}N936}$, pGEXKG-$Slo1_{I937\text{-}A985}$, pcDNA 3.1(−)-$Ca_v\beta1$, pcDNA 3.1(−)-$Ca_v\beta1_{M1\text{-}D224}$, and pcDNA 3.1(−)-$Ca_v\beta1_{P162\text{-}R598}$, were constructed in our laboratory using standard methods. The fidelity of all constructs was confirmed by sequencing. Mouse anti-Myc 9B11 and mouse anti-HA 2367 (Cell Signaling Technology Inc., Danvers, MA) were used for immunoblot analysis, whereas FITC-conjugated goat anti-Myc ab1263 (Abcam, Cambridge, MA) was used only for labeling of intracellular stores of Slo1 channels in confocal microscopy. Immunoblot and confocal analyses of endogenously expressed channel subunits were carried out with a rabbit antibody against mouse Slo1 (AB5228; Chemicon International, Temecula, CA) and a monoclonal antibody against $Ca_v\beta1$ (H00000782-M01; Abnova, Heidelberg, Germany), as described below.

Yeast Two-Hybrid Screen. This screen was carried out using the Matchmaker system (BD Biosciences, San Jose, CA) according to the manufacturer's instructions, as described in detail previously (Kim et al., 2007a). In brief, a cDNA library of embryonic day 9 (E9) chick ciliary ganglion (CG) prepared in our laboratory was screened using a construct encoding amino acids 785 to 985 of mouse Slo1 cloned into the pGBKT7 bait vector. Colonies expressing potential interacting proteins were identified by blue-white selection carried out on a quadruple dropout medium supplemented with 5-bromo-4-chloro-3-indolyl α-D-galactopyranoside. After selection, the pGADT7 plasmids encoding fragments of putative interacting proteins were isolated from yeast colonies, sequenced, and subjected to BLAST search analysis.

Coimmunoprecipitation, GST Pull-Down Assays, and in Vitro Binding Assays. Immunoblot analyses, coimmunoprecipitation, and glutathione transferase (GST) pull-down assays were carried out as described previously (Kim et al., 2007a). The in vitro binding assay is a slight modification of the GST pull-down assay. Full-length $Ca_v\beta1$ cDNA was cloned into the pcDNA3.1(−) vector for in vitro transcription and translation using the TNT T7 quick-coupled transcription/translation system (Promega, Madison, WI). Biotinylated lysine residues were incorporated into the in vitro translated protein using Trancend tRNA (Promega), which allowed for chemiluminescent detection of $Ca_v\beta1$ on nitrocellulose membranes using the Trancend nonradioactive detection system (Promega). Glutathione-Sepharose 4B beads carrying GST-fusion proteins prepared from Slo1 were incubated with in vitro-translated $Ca_v\beta1$ in PBS containing 0.2% Triton X-100 (PBST) overnight at 4°C with gentle rotation. The beads were washed repeatedly in PBST and eluted in a buffer containing 10 mM glutathione. Eluates were separated by 10% SDS-polyacrylamide gel electrophoresis, transferred to nitrocellulose membranes, and analyzed by addition of a streptavidin-horseradish peroxidase conjugate (1:10,000 dilution in a Tris-buffered saline containing 0.5% Tween 20) followed by detection of labeled proteins by chemiluminescence.

Cell Culture and Transfection. Human embryonic kidney (HEK) 293T cells were grown in Dulbecco's modified Eagle's medium (Sigma-Aldrich, St. Louis, MO) containing 10% heat-inactivated fetal bovine serum at 37°C in a 5% CO_2 incubator. Transfection procedures are described in Kim et al. (2007a). Cells were used for physiology or biochemistry 48 h after transfection. Neurons from E9 chick ciliary ganglia were dissociated and cultured as described previously (Cameron et al., 1998; Lhuillier and Dryer, 2002).

Immunostaining and Confocal Microscopy. E9 CG neurons were maintained in culture for 3 or 48 h, and then they were fixed in 4% paraformaldehyde for 10 min, blocked, and permeabilized with PBS containing 0.5% Triton X-100. The preparations were then incubated with rabbit anti-Slo1 (1:500 dilution) and mouse anti-$Ca_v\beta1$ (1:1000 dilution) overnight at 4°C. After repeated washing, cells were incubated with Alexa Fluor 488-conjugated anti-rabbit and cyanine 3-conjugated anti-mouse secondary antibodies for 1 h at 37°C, rinsed repeatedly in PBS, and mounted in Vectashield (Vector Laboratories, Burlingame, CA). Images were collected on an FV-1000 confocal microscope (Olympus, Tokyo, Japan) using a Plan Apo N 60× 1.42 numerical aperture oil immersion objective. Green fluorescence was evoked using an excitation wavelength of 495 nm, and emission was monitored at 519 nm. Red fluorescence was evoked by excitation at 580 nm, and emission was monitored at 620 nm.

Immunochemical Analysis of Cell Surface Slo1 Channels in HEK293T Cells. Intact HEK293T cells expressing Myc-tagged Slo1 channels in the presence or absence of $Ca_v\beta1$ were treated with

mouse anti-Myc (9B11l Cell Signaling Technology Inc.) for 20 min in normal culture medium at 37°C to label surface Slo1 channels. Cells were then rinsed in PBS, fixed in 4% paraformaldehyde for 10 min, permeabilized with PBST, blocked, and then labeled with cyanine 3-conjugated goat anti-mouse and FITC-conjugated goat anti-Myc (ab1263) for 1 to 2 h at room temperature. These tagged antibodies allowed visualization of surface (red fluorescence) and intracellular (green fluorescence) Slo1 channels, respectively, by confocal microscopy. Cell surface biotinylation assays were carried out as described in detail previously (Kim et al., 2007a,b,c). In brief, intact HEK293T cells were labeled with a membrane-impermeable biotinylation reagent [sulfosuccinimidyl 2-(biotinamido)-ethyl-1,3-dithiopropionates] (Pierce Biotechnology, Rockford, IL). Cells were then lysed, and biotinylated proteins from the cell surface were recovered by incubating lysates with streptavidin-agarose beads. A sample of the initial lysate was reserved to measure expression of total Slo1 proteins (surface + intracellular). All of the samples were separated by SDS-PAGE and analyzed by immunoblot using an antibody against the Myc tags on the Slo1 channels.

Electrophysiology and Statistics. All physiological experiments were conducted at room temperature. Recordings were made from red fluorescent HEK293T cells coexpressing Slo1 channels with red fluorescent protein (RFP)-tagged $Ca_v\beta1$ or with RFP. Inside-out patches were excised using standard methods. In brief, fire-polished glass micropipettes were filled with a solution containing 140 mM KCl, 1.2 mM $MgCl_2$, 14 mM glucose, and 10 mM HEPES, pH 7.2, and they had resistances of 2 to 5 MΩ after filling. Test solutions bathing the cytoplasmic face of the patch membrane contained 140 mM KCl, 1.2 mM $MgCl_2$, 14 mM glucose, 10 mM HEPES, pH 7.2, and <1 nM free Ca^{2+} buffered with 10 mM EGTA, or 1, 5, or 10 μM free Ca^{2+} buffered with 10 mM *N*-hydroxy-EDTA. The free Ca^{2+} concentrations in these solutions were checked using an Orion 97-20 calcium electrode (Thermo Fisher Scientific, Waltham, MA) calibrated with commercial solution standards obtained from WPI (Sarasota, FL). Currents in each test solution were evoked by a series of eight 450-ms depolarizing steps from a holding potential of −60 mV using an Axopatch 1D amplifier (Molecular Devices, Sunnyvale, CA). Currents were digitized, and then they were analyzed off-line using pCLAMP software (Molecular Devices). Because the potassium equilibrium potential in these conditions is 0 mV, large inward tail currents occur immediately after the break of the depolarizing step pulses, and some of the step commands (e.g., to −40 mV) also yield inward currents. Methods for whole-cell recordings of Slo1 currents in transiently transfected HEK293T cells have been described previously (Kim et al., 2007a,b,c). In brief, the bathing solution contained 150 mM NaCl, 0.08 mM KCl, 0.8 mM $MgCl_2$, 5.4 mM $CaCl_2$, and 10 mM HEPES, pH 7.4. The pipette solution contained 145 mM NaCl, 2 mM KCl, 6.2 mM $MgCl_2$, 10 mM HEPES, pH 7.2, and 5 μM free Ca^{2+} buffered with 10 mM *N*-hydroxy-EDTA. Note that with these solutions, the concentrations of K^+ inside and outside the cell are reduced to prevent whole-cell currents from saturating the patch-clamp amplifier, but the potassium equilibrium potential is physiological. Voltage activation curves in inside-out patches were generated from tail currents recorded at −60 mV by plotting the fractional activation ($I_{tail}/\bar{I}_{tail}$) against the voltage of the step command V used to evoke the currents, and then fitting the resulting curves with the Boltzmann function $I_{tail}/\bar{I}_{tail} = [1 + \exp(-(V - V_{1/2})qF/RT)]^{-1}$, where I_{tail} is the tail current amplitude evoked by pulse V, $\bar{I}_{tail}$ is the maximal tail current (determined from the traces in the patch evoked by steps to +80 mV in 10 μM Ca^{2+}), $V_{1/2}$ is the voltage of half-maximal activation, q is a slope constant, F is the Faraday constant, R is the gas constant, and T is absolute temperature. A descriptive time constant related to the kinetics of channel activation (τ_{act}) was obtained by fitting the rising phase of evoked currents with a single-exponential using the Levenberg-Marquardt algorithms implemented in Origin version 7.0 software (OriginLab Corp, Northampton, MA). We tested the hypothesis that the presence or absence of $Ca_v\beta1$ affects the Ca^{2+} sensitivity of the dependent variables $V_{1/2}$ or τ_{act} by two-way analysis of variance (ANOVA), with data from six patches in each group of cells. Other quantitative data are graphically presented as mean ± S.E.M. compiled from 10 to 25 cells in each group. Designs in which a single experimental group was compared with a single control group were analyzed using Student's unpaired t test. All statistical analyses were performed using STATISTICA software (Statsoft, Tulsa, OK), with $P < 0.05$ regarded as significant.

Methods for whole-cell recordings and quantification of Ca^{2+}-activated K^+ currents and voltage-activated Ca^{2+} currents from chick CG neurons have been described in detail previously (Dourado and Dryer, 1992; Cameron et al., 1998). In brief, the bath solution contained 145 mM NaCl, 5.3 mM KCl, 0.8 mM $MgCl_2$, 5.4 mM $CaCl_2$, 10 mM HEPES, and 250 nM tetrodotoxin, pH 7.4. Pipette solutions contained 120 mM KCl, 2 mM $MgCl_2$, 10 mM HEPES, and 10 mM EGTA, pH 7.2. For Ca^{2+}-free salines, all external Ca^{2+} was replaced on an equimolar basis with $MgCl_2$. Currents were evoked by step depolarizations from a holding potential of −40 mV, and net Ca^{2+}-dependent currents were calculated by digital subtractions (control − Ca^{2+}-free) and normalized for cell surface area as described previously (Dourado and Dryer, 1992). We have previously shown that all of the macroscopic outward currents observed under these conditions are carried by BK_{Ca} channels (Lhuillier and Dryer, 1999; Cameron and Dryer, 2000). The much smaller voltage-activated Ca^{2+} currents were measured using similar procedures, except that the bath also contained 250 nM tetrodotoxin, 10 mM tetraethylammonium, 5 mM 4-aminopyridine, and 2 μM ω-conotoxin, and KCl in the pipette solutions was replaced with CsCl. In the presence of ω-conotoxin, essentially all of the remaining Ca^{2+} current in ciliary neurons is carried by nifedipine-sensitive L-type channels (Wisgirda and Dryer, 1994).

Results

BK_{Ca} Channels Interacted Directly with $Ca_v\beta1$. To identify proteins that regulate BK_{Ca} channels, we conducted a yeast two-hybrid screen from an E9 chick CG cDNA library, using a bait from the cytoplasmic C-terminal (Gly785–Ala985) of Slo1 that is conserved in most splice variants. This bait region includes the calcium bowl (Thr911–Gln933) (Schreiber and Salkoff, 1997) and a portion of the regulator of conductance of K^+ 2 domain (Xia et al., 2002) (Fig. 1A). $Ca_v\beta1$ emerged repeatedly in this screen. We confirmed that Slo1 binds to $Ca_v\beta1$ by four independent methods. First, we observed that $Ca_v\beta1$ coimmunoprecipitates with native Slo1 channels when E9 CG extracts were probed with Slo1 antibodies (Fig. 1B). This also occurred in HEK293T cells coexpressing Myc-tagged Slo1 channels and HA-tagged $Ca_v\beta1$ subunits (Fig. 1C). HEK293T cells do not express endogenous voltage-activated Ca^{2+} channels; therefore, this result suggests that the interaction does not require the pore-forming subunits of voltage-activated Ca^{2+} channels. In addition, we carried out pull-down experiments to confirm the interaction. To do this, we prepared a GST-fusion protein encoding the bait (GST-$Slo1_{G785\text{-}A985}$), and we incubated it with chick CG extracts. We observed that GST-$Slo1_{G785\text{-}A985}$ could precipitate $Ca_v\beta1$ subunits from chick CG extracts that could be detected by immunoblot analysis, whereas GST was ineffective (Fig. 1D). In addition, we observed colocalization of endogenous $Ca_v\beta1$ and Slo1 subunits in cultured E9 CG neurons by confocal microscopy. Extensive colocalization of Slo1 (green fluorescence) and $Ca_v\beta1$ (red fluorescence) was readily detectable in merged images, and this seemed to occur in intracellular pools and on the plasma membrane (Fig. 1E, top, middle) in CG neurons processed 3 h after dissociation.

Colocalization of Slo1 and $Ca_v\beta1$ also occurred in neurites that extended from neuronal somata in cells maintained in culture for longer periods (Fig. 1E, bottom).

$Ca_v\beta1$ Physically Associated with Slo1 at Two Distinct Regions. To identify specific regions of Slo1 that interact with $Ca_v\beta1$, we made constructed smaller GST-fusion proteins made up of mutually exclusive regions within our initial Slo1 bait, shown schematically in Fig. 2A. We observed that GST-$Slo1_{T884\text{-}N936}$, which includes the calcium bowl (Thr911–Gln933), was able to precipitate $Ca_v\beta1$ from CG extracts, whereas GST, GST-$Slo1_{G785\text{-}L843}$, GST-$Slo1_{Q844\text{-}I883}$, and GST-$Slo1_{I937\text{-}A985}$ were ineffective (Fig. 2B). Recall that the calcium bowl region of Slo1 is required for a portion of high-affinity (micromolar) Ca^{2+} binding and activation of BK_{Ca} channels (Bao et al., 2002; Zeng et al., 2005). We also looked for potential $Ca_v\beta1$ binding sites outside the portions of Slo1 that we used for our bait. Because $Ca_v\beta1$ has a functional SH3 domain (Tian et al., 2006), we prepared a GST-fusion protein that includes the noncanonical SH3-binding motifs of Slo1 (GST-$Slo1_{E637\text{-}D677}$). This fusion protein was also able to precipitate $Ca_v\beta1$ from chick CG extracts (Fig. 2B). These interactions were observed in extracts of neuronal cells that express a full complement of voltage- and ligand-gated channels, and they cannot exclude Slo1-$Ca_v\beta1$ interactions that occur as part of a larger complex. To address that issue, we placed human $Ca_v\beta1$ cDNA into pcDNA3.1(−) vector, and we translated it in vitro with incorporated biotinylated lysine residues to facilitate detection. The purified product was then added to various purified GST-Slo1-fusion proteins as binary mixtures. We observed that $Ca_v\beta1$ interacted directly with GST-$Slo1_{T884\text{-}N936}$ and GST-$Slo1_{E637\text{-}D677}$ but not with the other GST-Slo1-fusion proteins (Fig. 2C). From these results, we conclude that Slo1-$Ca_v\beta1$ interactions do not require contributions from other proteins.

$Ca_v\beta1$ Affected BK_{Ca} Gating by Reducing Its Sensitivity to Ca^{2+}. The functional significance of Slo1-$Ca_v\beta1$ interactions was examined in inside-out patches excised from HEK293T cells expressing one or both of these channel subunits. For these experiments, we placed the cDNA encoding

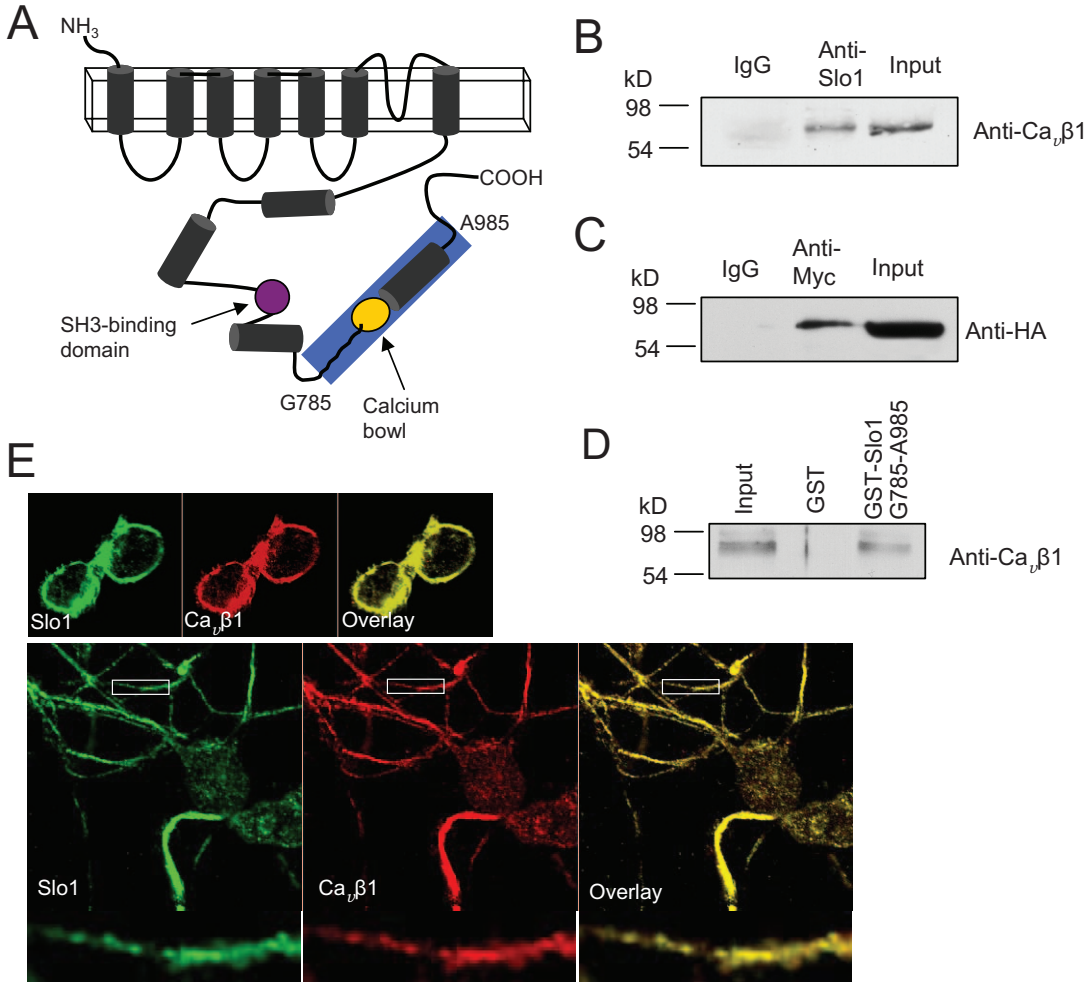

Fig. 1. Direct interaction between $Ca_v\beta1$ and the calcium bowl and SH3 domain-binding motifs of Slo1. A, schematic representation of Slo1. The bait fragment used in the yeast-two hybrid screen is highlighted in blue. The calcium bowl and a noncanonical SH3-binding domain are indicated in yellow and magenta, respectively. B, coimmunoprecipitation of $Ca_v\beta1$ and Slo1 from chick ciliary ganglion extracts. C, coimmunoprecipitation of $Ca_v\beta1$ and Slo1 from extracts of HEK293T cells expressing Myc-Slo1 and HA-$Ca_v\beta1$ after transient transfection. D, GST pull-down assays carried out on chick ciliary ganglion lysates show that GST-$Slo1_{G785\text{-}A985}$ binds to $Ca_v\beta1$. E, colocalization of $Ca_v\beta1$ and Slo1 in E9 chick ciliary ganglion neurons kept in dissociated cell culture for 3 h (top) or 2 days (middle). Regions of neurites outlined by white boxes are shown at a higher magnification on the bottom panels.

human $Ca_v\beta1$ subunit into the pDsRed2-N1 expression vector, which allows for expression of $Ca_v\beta1$ with a C-terminal RFP tag. Control cells expressed RFP. Voltage-evoked currents in symmetrical 140 mM KCl were recorded in patches excised from HEK293T cells expressing Slo1 in the presence or absence of $Ca_v\beta1$-RFP. When either $Ca_v\beta1$-RFP or RFP was expressed alone in HEK293T cells, the RFP tag was found throughout the cell, and we did not detect voltage-evoked currents in excised inside-out patches (data not shown). Coexpression of Slo1 with RFP yielded robust Ca^{2+}- and voltage-dependent currents similar to those observed by others (Fig. 3). However, coexpression of Slo1 and $Ca_v\beta1$-RFP resulted in families of currents with substantially slower activation kinetics than those observed when Slo1 was expressed by itself (Fig. 3, A–C). This was analyzed by fitting the rising phase of currents recorded at +80 mV as a single exponential and then comparing the resulting τ_{act} in patches from control and cotransfected HEK293T cells exposed to three different concentrations of Ca^{2+} (Fig. 3C). These data were analyzed by two-way ANOVA. We observed significant effects of $Ca_v\beta1$-RFP ($F_{30} = 66.44215$, $P < 0.0001$) and Ca^{2+}($F_{30} = 32.47008$, $P < 0.0001$) on the kinetics of activation. More importantly, there was a statistically significant interaction effect between the effects Ca^{2+} concentration and channel stoichiometry on the resulting activation kinetics ($F_{30} = 8.62344$, $P < 0.01$), suggesting that the $Ca_v\beta1$ subunit regulates the sensitivity of Slo1 channels to Ca^{2+}. A similar conclusion emerged from analyses of activation curves constructed from measurements of tail current amplitudes evoked by families of voltage steps applied in the presence of different bath Ca^{2+} concentrations (Fig. 3, D and E). Increasing bath Ca^{2+} caused a significant ($F_{30} = 17.53$, $P < 0.0003$) shift in the $V_{1/2}$ to more negative membrane potentials in control cells expressing Slo1 alone. There was also a significant effect of Ca^{2+} on the $V_{1/2}$ for activation in cells coexpressing $Ca_v\beta1$ ($F_{30} = 60.836$, $P < 0.00001$). However, the resulting BK_{Ca} channels seemed to be less sensitive to Ca^{2+} than control channels, and there was a statistically significant interaction effect between the response to Ca^{2+} and the presence of $Ca_v\beta1$ ($F_{30} = 6.159$, $P < 0.0057$). This can be readily seen by comparing the mean $V_{1/2}$ for channel activation obtained at 5 μM Ca^{2+} in the two groups, which is statistically significant ($P < 0.05$) by Scheffé's post hoc test (Fig. 3E). This pattern suggests a reduction in the sensitivity of Slo1 to Ca^{2+} in the presence of $Ca_v\beta1$, possibly because this subunit binds close to or within the calcium bowl domains of Slo1.

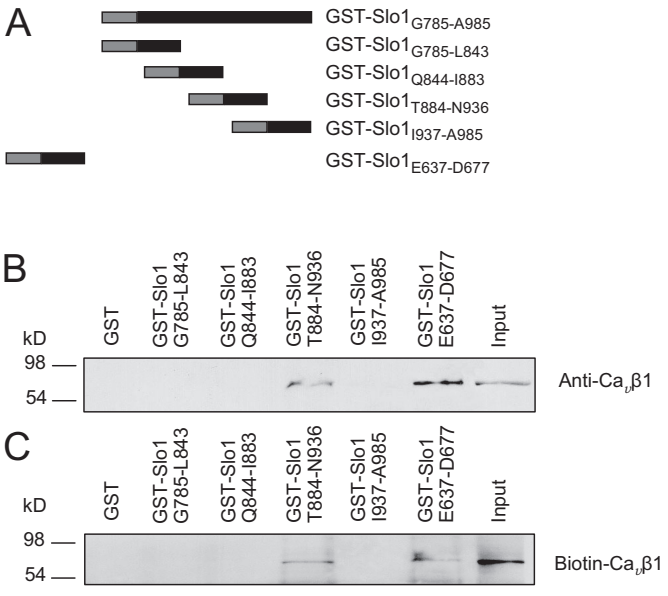

Fig. 2. Interactions between $Ca_v\beta1$ and Slo1 do not require the presence of additional proteins. A, schematic representation of GST-fusion protein constructs encoding GST-$Slo1_{G785\text{-}A985}$, GST-$Slo1_{G785\text{-}L843}$, GST-$Slo1_{Q844\text{-}I883}$, GST-$Slo1_{T884\text{-}N936}$, GST-$Slo1_{I937\text{-}A985}$, and GST-$Slo1_{E637\text{-}D677}$. B, GST pull-down assays show that GST-$Slo1_{I937\text{-}A985}$ and GST-$Slo1_{E637\text{-}D677}$ bind to $Ca_v\beta1$ in chick ciliary ganglion extracts. C, full-length biotin-$Ca_v\beta1$ binds directly to GST-$Slo1_{I937\text{-}A985}$ and GST-$Slo1_{E637\text{-}D677}$ in a binary mixture. No other proteins were present in the assay.

We observed similar effects of $Ca_v\beta1$ on the amplitudes and kinetics of whole-cell currents recorded with pipettes containing 5 μM free Ca^{2+} from transfected HEK293T cells using methods described previously. The voltage-evoked currents recorded from cells coexpressing Slo1 and $Ca_v\beta1$-RFP were markedly different from those observed in cells coexpressing Slo1 and RFP (Fig. 4A). In particular, currents were markedly reduced in amplitude, and they were significantly slower in $Ca_v\beta1$-RFP-cotransfected cells (Fig. 4, B and C), much as was seen with inside-out patches exposed to the same concentration Ca^{2+}.

Overexpression of $Ca_v\beta1$ Inhibited Ca^{2+}-Activated K^+ Currents and Potentiateed L-Type Ca^{2+} Currents in Native Neurons. To study the implications of Slo1-$Ca_v\beta1$ interactions in native conditions, we examined the effects of overexpressing $Ca_v\beta1$ chick CG neurons placed in culture on E9. Stabilized cultures were transiently transfected with either $Ca_v\beta1$-RFP or RFP, and whole-cell currents were recorded from fluorescent cells 48 h later using methods that we have used for many years to isolate Ca^{2+}-activated K^+ currents or voltage-activated Ca^{2+} currents (Cameron et al., 1998). The effects of $Ca_v\beta1$ were similar to those seen in HEK293T cells. In particular, there was a statistically significant reduction in the mean amplitude of Ca^{2+}-activated K^+ currents in CG neurons transfected with $Ca_v\beta1$-RFP compared with those observed in cells transfected with RFP (Fig. 5, A and B). The rising phase of macroscopic Ca^{2+}-dependent K^+ currents was also substantially slower, much as we observed in HEK293T cells expressing $Ca_v\beta1$. By contrast, we observed significant potentiation of endogenous voltage-activated Ca^{2+} currents in $Ca_v\beta1$-RFP transfected CG neurons compared with those seen in cells expressing RFP (Fig. 5, C and D). We observed that $Ca_v\beta1$ expression also caused a slight left shift in the voltage dependence of Ca^{2+} currents (Fig. 5E).

$Ca_v\beta1$ Had No Effect on Surface Expression of Slo1. Although the above-mentioned experiments establish an effect of $Ca_v\beta1$ on Slo1 gating, they do not address the possibility that this subunit influences the steady-state surface expression of Slo1. We addressed this issue in three different types of experiments. First, there was no significant difference in average maximal outward currents evoked by voltage steps to +60 mV in the presence of 20 μM bath Ca^{2+} in inside-out patches excised from HEK293T cells expressing Slo1 in combination with either RFP or $Ca_v\beta1$-RFP (Fig. 6A). Current differences in these recording conditions are likely to reflect the number of functional channels in the plasma membrane. In addition, we examined the surface expression of Slo1 channels in HEK293T cells in the presence and ab-

sence of $Ca_v\beta1$ by labeling surface Slo1 channels in live cells with FITC-conjugated anti-Myc antibody (green). The cells were then fixed, blocked, permeabilized, and labeled with a nonconjugated anti-Myc raised in a different species to obtain signal from intracellular Slo1 channels (red). The distribution of channels was then determined by confocal microscopy, using the same laser intensities for all measurements. The resulting images suggest that coexpression of $Ca_v\beta1$ had no effect on the surface expression of Slo1 (Fig. 6B). In addition, we carried out cell surface biotinylation assays in HEK293T cells expressing Myc-tagged Slo1 channels in the presence or absence of HA-tagged $Ca_v\beta1$, and we observed no quantitative difference in the amounts of total or cell surface Slo1 (Fig. 6C). From these data, we conclude that $Ca_v\beta1$ primarily affects the gating properties of BK_{Ca} channels and that the effects on macroscopic current amplitude in native cells and in heterologous expression systems are not caused by significant effects on steady-state surface expression of Slo1.

Interactions with the GK Domain of $Ca_v\beta1$ Were Sufficient to Modulate BK_{Ca} Gating. Recent structural analyses of the family of $Ca_v\beta$ subunits have demonstrated that an SH3 domain and a GK domain form a bidentate interaction with the pore-forming subunits of L-type Ca^{2+} channels, resulting in changes in their gating, trafficking and stability in the plasma membrane (Takahashi et al., 2005). The noncatalytic GK domain is a structural signature of the membrane-associated guanylate kinase family of proteins, and it is a potential protein-protein interaction motif (Chen et al., 2004; Van Petegem et al., 2004) (Fig. 7A). To identify the regions in $Ca_v\beta1$ that interact with Slo1, we carried out in vitro binding assays in binary mixtures of GST-Slo1-fusion proteins and two different purified $Ca_v\beta1$ fragments. The latter include $Ca_v\beta1_{M1\text{-}D224}$ and $Ca_v\beta1_{P162\text{-}R598}$, which com-

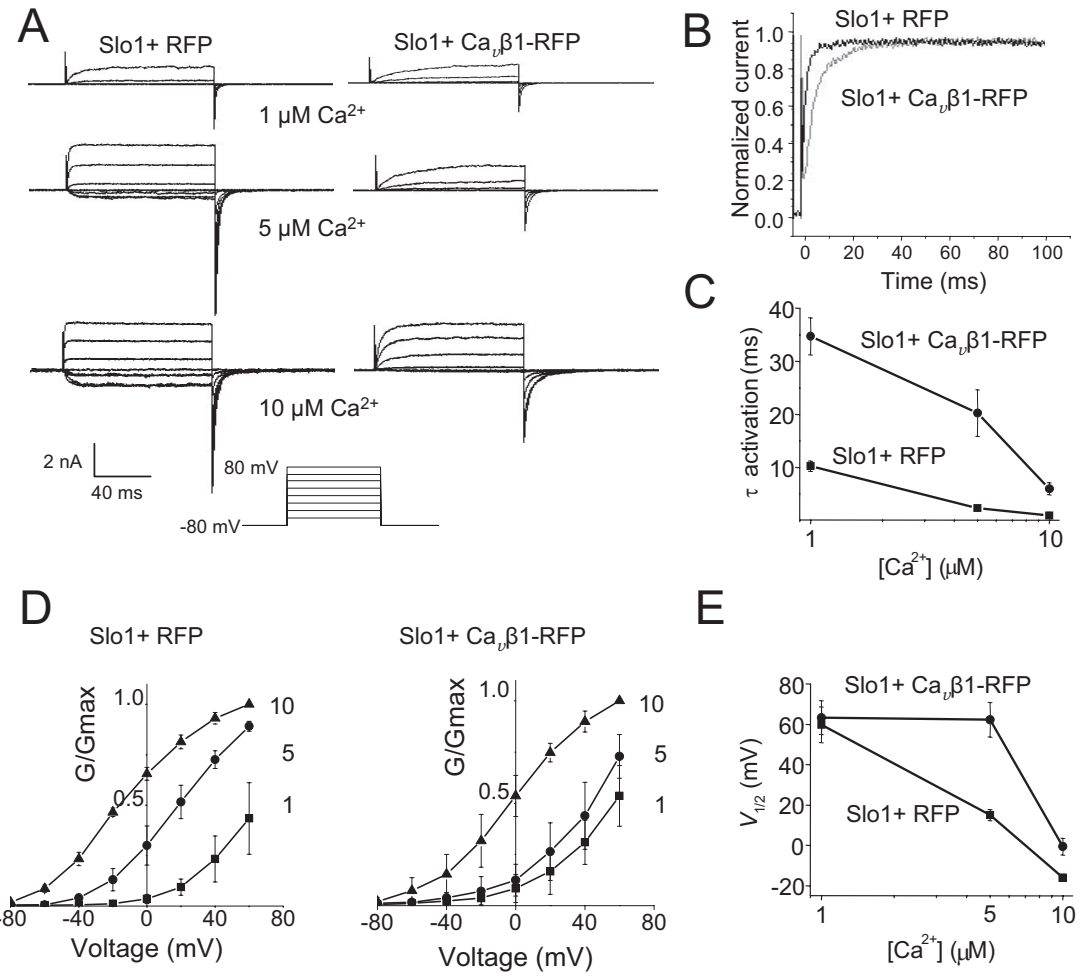

Fig. 3. $Ca_v\beta1$ modulates the gating properties of BK_{Ca} channels. Inside-out patch were excised from HEK293T cells expressing Slo1 in the presence or absence of $Ca_v\beta1$. A, representative families of currents evoked by voltage steps (−80 to +80 mV) in inside-out patches at different bath Ca^{2+} concentrations, as indicated. No currents were detected in Ca^{2+}-free bath solutions (data not shown). Note slower kinetics in presence of $Ca_v\beta1$. B, rising phase of currents evoked by a voltage step to +80 mV in the presence of 10 μM Ca^{2+}. These are plotted so as to facilitate comparisons of activation kinetics. C, rising phase of these types of evoked currents were fitted with single-exponential curves, and the resulting time constants were plotted against bath Ca^{2+}. Increasing bath Ca^{2+} causes channels to activate more rapidly. Two-way ANOVA of this data set reveals a significant ($P < 0.0001$) interaction effect, indicating that the presence of $Ca_v\beta1$ affects the Ca^{2+} sensitivity of the resulting activation kinetics. Error bars are S.E.M. D, voltage-activation curves of Slo1 and Slo1 + $Ca_v\beta1$ channels obtained at different bath Ca^{2+} concentrations constructed from the tail currents recorded from inside-out patches, readily seen in A. Data points (mean ± S.E.M.) are shown with superimposed fitted Boltzmann curves. Bath Ca^{2+} concentrations (in micromolar) are indicated next to the corresponding curves. E, plot of the $V_{1/2}$ values derived from Boltzmann fits at different bath Ca^{2+} concentrations for Slo1 and Slo1 + $Ca_v\beta1$ channels. These data were analyzed by two-way ANOVA, which revealed a significant interaction effect between the response to Ca^{2+} and the presence of $Ca_v\beta1$ ($P < 0.0057$).

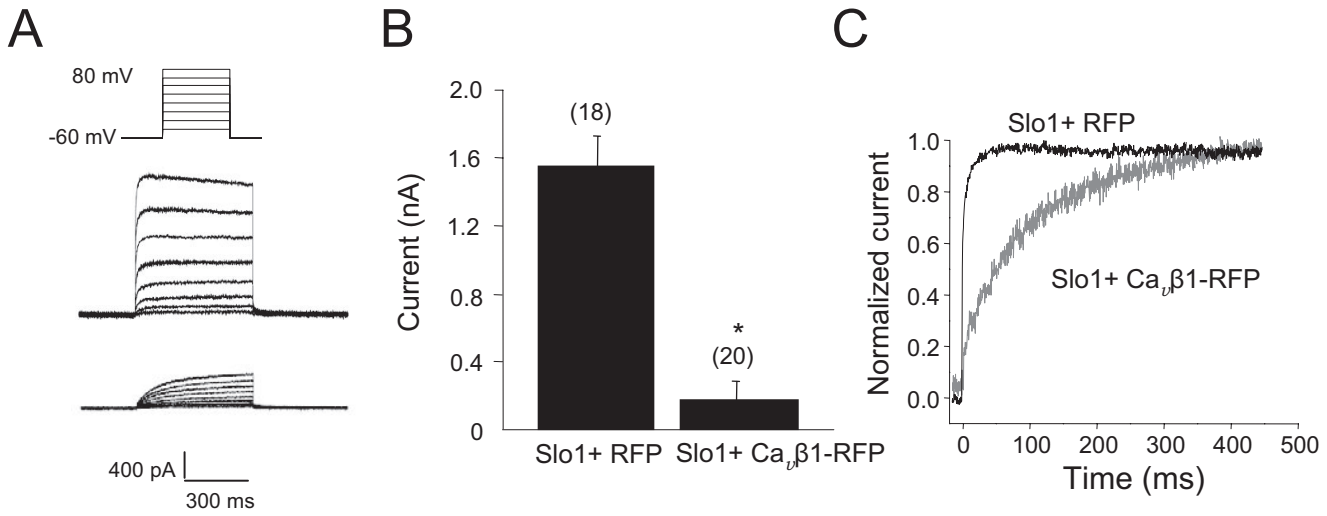

Fig. 4. Whole-cell currents from HEK293T cells expressing Slo1 in the presence or absence of RFP-tagged $Ca_v\beta1$. A, families of voltage-evoked whole-cell currents in transfected HEK293T cells coexpressing Slo1 and RFP (top) or Slo1 and $Ca_v\beta1$-RFP (bottom). The recording pipettes contained 5 μM Ca^{2+}. Note smaller and slower currents in presence of $Ca_v\beta1$-RFP. B, bar graph shows mean ± S.E.M. of the maximal whole-cell currents evoked by steps to +80 mV. Cells coexpressing RFP-$Ca_v\beta1$ have significantly smaller currents ($P < 0.01$ by Student's unpaired t test). C, effect of $Ca_v\beta1$ on the rising phase of representative whole-cell currents evoked by a step to +80 mV plotted so as to facilitate comparison of activation kinetics.

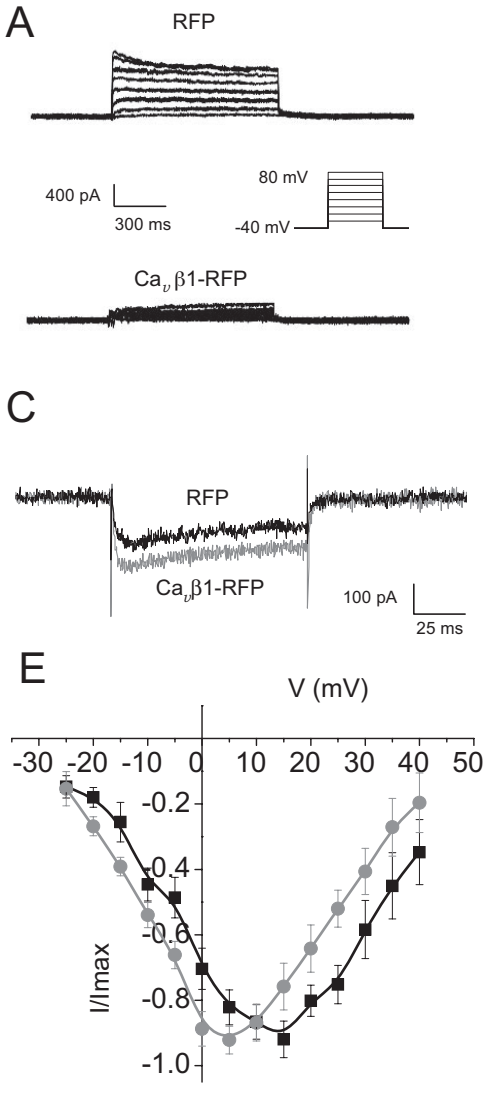

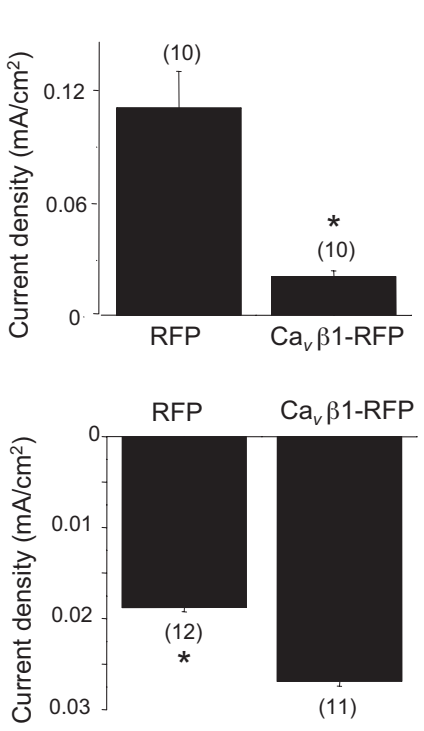

Fig. 5. Overexpression of $Ca_v\beta1$ affects macroscopic Ca^{2+}-dependent K^+ currents and voltage-activated Ca^{2+} currents in chick CG neurons. Whole-cell currents were evoked by a series of depolarizing voltage steps in the presence and absence of external Ca^{2+}, and net Ca^{2+}-dependent currents were obtained by digital subtraction. A, families of Ca^{2+}-dependent voltage-evoked K^+ currents in CG neurons overexpressing RFP or $Ca_v\beta1$-RFP. Note smaller and slower currents in $Ca_v\beta1$-RFP-transfected neurons. B, mean ± S.E.M. of the maximal Ca^{2+}-dependent outward currents evoked by steps to +80 mV from a holding potential of −40 mV. Current densities were significantly smaller when $Ca_v\beta1$-RFP was present ($P < 0.01$ by student's unpaired t test). C, comparison of voltage-evoked maximal whole cell L-type calcium currents recorded from neurons expressing RFP or $Ca_v\beta1$-RFP, as indicated. The recording electrodes contained 150 mM CsCl and external solutions contained 0.1 μM tetrodotoxin, 10 mM tetraethylammonium, and 2 μM ω-conotoxin. D, mean ± S.E.M. of the maximal L-type current densities evoked from a holding potential of −40 mV. Current densities were significantly smaller in cells overexpressing $Ca_v\beta1$-RFP compared with cells overexpressing RFP ($P < 0.01$ by Student's unpaired t test). E, normalized current-voltage relationship of L-type Ca^{2+} currents in CG neurons overexpressing RFP (black) or $Ca_v\beta1$-RFP (gray). Data points are mean ± S.E.M. from eight cells in each group, and the curves are spline fits with no theoretical significance.

prise the SH3 and GK domains, respectively. We observed that $Ca_v\beta1_{M1\text{-}D224}$ binds to GST-$Slo1_{E637\text{-}D677}$, a region within Slo1 that contains a noncanonical SH3-binding motif (Tian et al., 2006). We also observed that $Ca_v\beta1_{P162\text{-}R598}$ binds to GST-$Slo1_{T884\text{-}N936}$, which includes the calcium bowl domain (Fig. 7B). To examine the functional significance of these interactions, we expressed the $Ca_v\beta1$ fragments as RFP-fusion proteins in HEK293T cells, along with full-length Slo1. We then examined Slo1 gating in red fluorescent cells using whole-cell recordings with pipettes containing 5 μM Ca^{2+}, as described above. We observed that coexpression of RFP-$Ca_v\beta1_{P162\text{-}R598}$ caused slowing and inhibition of Slo1 currents similar to that observed with full-length RFP-$Ca_v\beta1$, whereas RFP-$Ca_v\beta1_{M1\text{-}D224}$ had no apparent effect on these parameters of Slo1 gating (Fig. 7, C and D). This suggests that interactions with the GK domain region of $Ca_v\beta1$ are sufficient to modulate BK_{Ca} gating.

Discussion

In many excitable cells, BK_{Ca} channels are components of a feedback system that limits the amount of Ca^{2+} influx evoked by membrane depolarization. Because of these dynamics, BK_{Ca} channels can contribute to spike repolarization, membrane potential oscillations, and the control of muscle contractility (Salkoff et al., 2006). Several investigators have addressed the question of how BK_{Ca} channels can be selectively regulated by Ca^{2+} influx through Ca_v channels given that BK_{Ca} channels typically require micromolar concentrations of free Ca^{2+} for robust activation at physiological membrane potentials (Grunnet and Kaufmann, 2004; Berkefeld et al., 2006; Loane et al., 2007). These studies have shown that complexes made up of the pore-forming α-subunits of BK_{Ca} channels (Slo1) and voltage-activated Ca^{2+} channels ($Ca_v1.2$, $Ca_v2.1$, and $Ca_v2.2$) can be copurified from

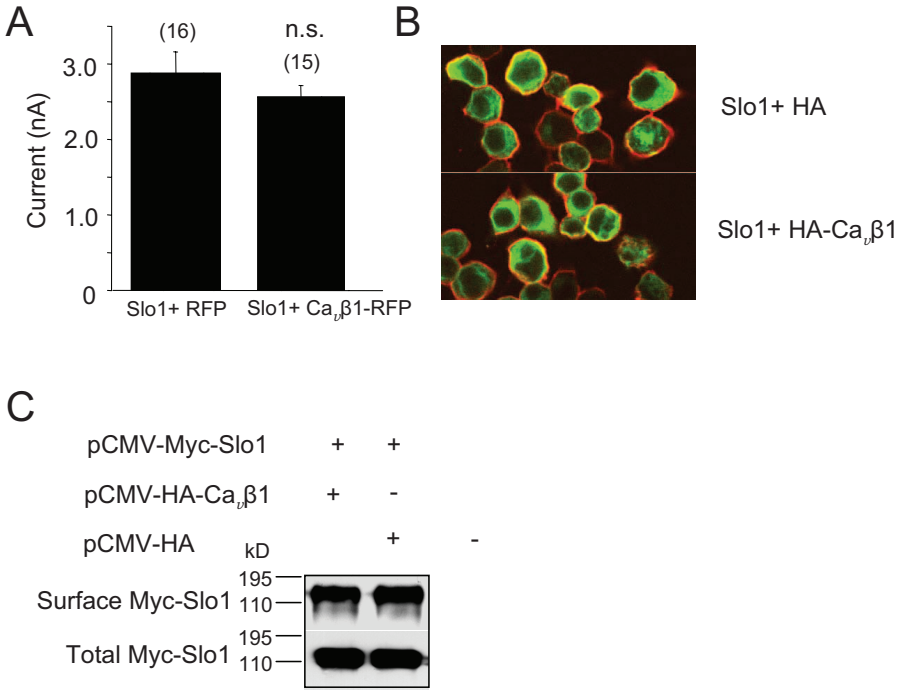

Fig. 6. Coexpression of $Ca_v\beta1$ does not alter steady-state levels of Slo1 on the surface of HEK293T cells. A, mean maximal currents (+60 mV and 10 μM Ca^{2+}) in inside-out patches excised from HEK293T cells coexpressing Slo1 and RFP or Slo1 and $Ca_v\beta1$-RFP are not significantly different. B, confocal images of the distribution of Slo1 channels in transfected HEK293T cells obtained using different primary antibodies against ectofacial Myc tags on Slo1 applied before and after cell permeabilization. Note that $Ca_v\beta1$ has no effect on surface expression of Slo1 (green fluorescence) or on Slo1 channels in intracellular pools (red fluorescence). The same laser intensities were used to obtain these images. C, cell-surface biotinylation assay using antibodies against the Myc tags on Slo1 shows no significant effect of $Ca_v\beta1$ on the surface expression of Slo1.

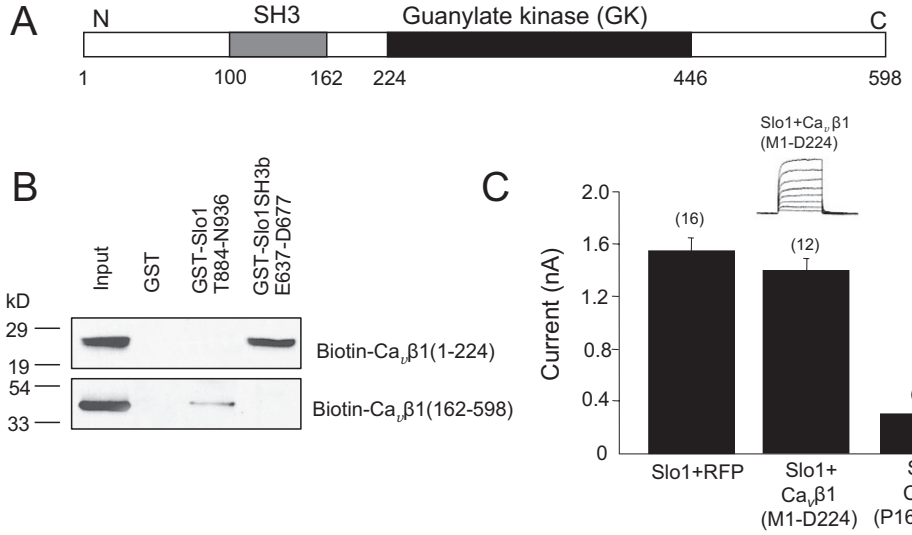

Fig. 7. The GK and SH3 domains of $Ca_v\beta1$ interact with Slo1, and the GK domain is necessary and sufficient to affect Slo1 gating. A, schematic diagram of $Ca_v\beta1$. The SH3 and GK domains are shown in gray and black, respectively. B, in vitro binding assay showing that the $Ca_v\beta1_{M1\text{-}D224}$ fragment, which includes the SH3 domain, binds to a noncanonical SH3-binding motif in Slo1 (Tian et al., 2006). A fragment comprised of $Ca_v\beta1_{P162\text{-}R598}$, which includes the GK domain, binds to the calcium bowl region of Slo1. C, whole-cell recordings from HEK293T cells made with recording pipettes containing 5 μM Ca^{2+} show that the $Ca_v\beta1_{P162\text{-}R598}$ fragment inhibits and slows macroscopic currents carried by Slo1. However, the $Cav\beta1_{M1\text{-}D224}$ fragment does not. Bar graphs represent mean ± S.E.M. Inset shows representative traces from HEK293T cells coexpressing the SH3-domain fragment.

mammalian brain. Although these complexes can include auxiliary (nonpore-forming) subunits of BK_{Ca} channels (β2 and β4) and Ca_v channels ($Ca_v\beta$1, $Ca_v\beta$2, $Ca_v\beta$3, and $Ca_v\beta$4) (Berkefeld et al., 2006), the auxiliary subunits are not necessary for BK_{Ca} channels to reside within the local (~20 nm) and steep Ca^{2+} concentration gradient that builds up around an open Ca_v channel pore in the presence of mobile buffers (Loane et al., 2007). Moreover, not all cell surface BK_{Ca} channels in neural cells occur in a complex with functional Ca_v channels (Gola and Crest, 1993; Marrion and Tavalin, 1998) and the potential consequences of formation Slo1-$Ca_v\beta$ complexes in which the pore-forming α-subunits of Ca^{2+} channels are missing have not been examined previously.

In the present study, we have observed a functionally significant interaction between Slo1 (BK_{Ca} channel) and $Ca_v\beta$1 subunits that can occurs in the absence of other proteins and that has a profound effect on the gating properties of BK_{Ca} channels. Formation of a complex with $Ca_v\beta$1 markedly slows voltage-evoked activation of BK_{Ca} channels, and it reduces their apparent Ca^{2+} sensitivity, leading to net inhibition of gating at moderate concentrations of cytoplasmic Ca^{2+}. It is important to note that this can occur in the absence of any other Ca_v channel subunits. In addition, we observed that coexpression of $Ca_v\beta$1 subunits did not have a marked effect on the steady-state surface expression of Slo1 subunits as detected by electrophysiology or biochemistry in HEK293T cells.

Previous studies have shown that $Ca_v\beta$ subunits interact with a conserved domain in the pore-forming α-subunits of Ca_v channels known as the α-interaction domain (Chen et al., 2004). The α-interaction domain interacts primarily with the GK domains of $Ca_v\beta$ subunits (Chen et al., 2004), and coexpression of a fragment containing only a portion of the GK domain is sufficient to cause shifts in the voltage dependence and kinetics of Ca_v channels (Chen et al., 2004). However, complete reconstitution of all of the modulatory activities of $Ca_v\beta$ subunits, including stimulation of trafficking, occurred only when fragments separately made up of SH3 and GK domains were simultaneously coexpressed with Ca_v α-subunits in HEK293 cells (Takahashi et al., 2005). The situation with Slo1 channels is somewhat different, because both of the protein interaction domains of $Ca_v\beta$1 can bind to Slo1 channels, although they do so at different sites in the cytoplasmic C-terminal of the latter. Moreover, expression of a fragment that contained only the GK domain was sufficient to reproduce the modulatory effects of full-length $Ca_v\beta$1 on the Ca^{2+}-dependent gating properties of BK_{Ca} channels. It is noteworthy that the GK domain of $Ca_v\beta$1 interacts at a site close to or within the calcium bowl domain of Slo1, a region necessary for at least a portion of high-affinity activation of BK_{Ca} channels by Ca^{2+} (Bao et al., 2002; Zeng et al., 2005). The calcium bowl domain seems to be especially important in regulating the kinetics of Ca^{2+}-dependent Slo1 channel activation at low (1–10 μM) Ca^{2+} concentrations (Zeng et al., 2005), and it is notable that one of the largest effects of $Ca_v\beta$1 is to slow activation of coexpressed Slo1 channels over that same concentration range. It is possible that binding of the $Ca_v\beta$1 GK domain to Slo1 modulates Ca^{2+} activation by simple steric hindrance within the calcium bowl, or through an allosteric mechanism that entails conformational changes in the overall Ca^{2+} binding pocket in that part of the Slo1 channel. Expression of the SH3 domain of $Ca_v\beta$1 by itself did not affect Ca^{2+}-dependent gating of Slo1 channels, but we cannot exclude that the SH3 domain plays a role in modulating other aspects of Slo1 function, possibly by allowing formation of a larger complex. In this regard, Slo1 channels have a noncanonical SH3-binding motif that has been implicated in cytoskeletal interactions that contribute to stretch-sensitive gating (Tian et al., 2006). It is possible that $Ca_v\beta$1 forms a bridge that allows mechanical coupling between SH3-binding motif and the calcium bowl, thereby contributing to the process of stretch-sensitive gating.

One question that emerges is whether $Ca_v\beta$1 subunits are independent targets of physiological regulation. As already noted, the portions of $Ca_v\beta$1 that produce functional effects upon binding to Slo1 are located within the GK domain, and the crystallographic data suggest that these sites may be occluded in those $Ca_v\beta$1 subunits that are already bound to Ca_v α-subunits (Chen et al., 2004). This suggests that under most conditions, interactions between $Ca_v\beta$ and Ca_v α-subunits predominate, and this is supported by the observation that Slo1 channels expressed in the presence of a combination of $Ca_v\beta$1 and Ca_v α-subunits have fast kinetics, similar to those observed when Slo1 is expressed by itself (Berkefeld et al., 2006), an observation that we have confirmed (S. Jha and S. E. Dryer, unpublished observations). Moreover, the fact that $Ca_v\beta$1 subunits can stimulate the surface expression of Ca_v α-subunits suggests that all high threshold voltage-activated Ca^{2+} channels are assembled with a β-subunit before insertion into the plasma membrane. However, it is possibly that these dynamics can be altered by changes in the relative abundance of the various subunits, but currently, very little is known about factors that regulate Cavβ at the transcriptional or translational level. However, it is worth noting that dynamin, a protein involved in endocytotic regulation of membrane-associated proteins, can bind to the SH3 domains of $Ca_v\beta$1 even in the absence of other subunits (Gonzalez-Gutierrez et al., 2007). In addition, several members of the Rad, Gem, and Kir family of Ras-like GTPases can also interact directly with the GK domains of $Ca_v\beta$1 subunits, leading to down-regulation of their steady-state expression on the cell surface (Béguin et al., 2001). Thus, it is possible that the amounts of $Ca_v\beta$1 at the cell surface are regulated independently of other subunits and that their removal from the plasma membrane exposes protein interaction motifs that allow them to form new interactions (e.g., with Slo1).

The present data argue against a role for $Ca_v\beta$1 in regulation of the trafficking of Slo1 channels, although it should be noted that this process is sometimes cell type-dependent, and HEK293T cells may not have provided the appropriate context in which to observe such an effect. Conversely, increases in the surface expression of $Ca_v\beta$1 could increase voltage-evoked Ca^{2+} influx by potentiation of Ca_v channels, and by independently slowing and inhibiting BK_{Ca} channels, thereby suppressing the main negative feedback to voltage-dependent Ca^{2+} influx. In this regard, the effect of $Ca_v\beta$1 subunits on BK_{Ca} channels is not saturated under normal physiological conditions, because overexpression of $Ca_v\beta$1 in native ciliary ganglion neurons caused slowing and reduction in mean densities of macroscopic Ca^{2+}-activated K^+ channels, along with a simultaneous increase in L-type Ca^{2+} currents. Finally, we should note that all of our experiments have been carried out on $Ca_v\beta$1 subunits, which normally

contribute to formation of L-type Ca^{2+} channels. The question arises as to whether other $Ca_v\beta$ subunits can produce a similar effect on Slo1. Although we have no data to address this issue, the GK domains of this group of proteins are very highly conserved (Dolphin, 2003); therefore, it is quite possible that this is a general property of all of them. This is notable because interactions between other Cavβ subunits and Slo1 have been described in brain (Berkefeld et al., 2006; Loane et al., 2007).

In summary, we have identified a functionally significant interaction between $Ca_v\beta1$, an auxiliary subunit of a voltage-activated Ca^{2+} channel, and Slo1 the principle pore-forming subunit of large-conductance Ca^{2+}-activated K^+ channels. Binding of $Ca_v\beta1$ to Slo1 can occur in the absence of any other channel subunits, and the interaction produced profound affects on the Ca^{2+}-dependent gating of BK_{Ca} channels. This interaction may comprise part of a mechanism to modulate negative feedback control of voltage-dependent Ca^{2+} influx in excitable cells.

Acknowledgments

We thank Dr. Min Li for providing Myc-tagged Slo1-expression constructs.

References

Bao L, Kaldany C, Holmstrand EC, and Cox DH (2004) Mapping the BK_{Ca} channel's "Ca^{2+} bowl": side-chains essential for Ca^{2+} sensing. *J Gen Physiol* **123:**475–489.

Bao L, Rapin AM, Holmstrand EC, and Cox DH (2002) Elimination of the BK_{Ca} channel's high-affinity Ca^{2+} sensitivity. *J Gen Physiol* **120:**173–189.

Béguin P, Nagashima K, Gonoi T, Shibasaki T, Takahashi K, Kashima Y, Ozaki N, Geering K, Iwanaga T, and Seino S (2001) Regulation of Ca^{2+} channel expression at the cell surface by the small G protein kir/Gem. *Nature* **411:**701–706.

Berkefeld H, Sailer CA, Bildl W, Rohde V, Thumfart JO, Eble S, Klugbauer N, Reisinger E, Bischofberger J, Oliver D, et al. (2006) BK_{Ca}-Ca_v channel complexes mediate rapid and localized Ca^{2+} activated K^+ signaling. *Science* **314:**615–620.

Bichet D, Lecomte C, Sabatier JM, Felix R, and De Waard M (2000) Reversibility of the Ca^{2+} channel $\alpha1$-β subunit interaction. *Biochem Biophys Res Commun* **277:** 729–735.

Brice NL, Berrow NS, Campbell V, Page KM, Brickley K, Tedder I, and Dolphin AC (1997) Importance of the different β subunits in the membrane expression of the α1A and α2 calcium channel subunits: studies using a depolarisation-sensitive α1A antibody. *Eur J Neurosci* **9:**749–759.

Cameron JS and Dryer SE (2000) BK-Type K_{Ca} channels in two parasympathetic cell types: differences in kinetic properties and developmental expression. *J Neurophysiol* **84:**2767–2776.

Cameron JS, Lhuillier L, Subramony P, and Dryer SE (1998) Developmental regulation of neuronal K^+ channels by target-derived TGFβ in vivo and in vitro. *Neuron* **21:**1045–1053.

Chen YH, Li MH, Zhang Y, He LL, Yamada Y, Fitzmaurice A, Shen Y, Zhang H, Tong L, and Yang J (2004) Structural basis of the $\alpha1$-β subunit interaction of voltage-gated Ca^{2+} channels. *Nature* **429:**675–680.

De Waard M, Pragnell M, and Campbell KP (1994) Ca^{2+} channel regulation by a conserved β subunit domain. *Neuron* **13:**495–503.

Díaz L, Meera P, Amigo J, Stefani E, Alvarez O, Toro L, and Latorre R (1998) Role of the S4 segment in voltage-dependent calcium sensitive potassium (hSlo1) channel. *J Biol Chem* **273:**32430–32436.

Dolphin AC (2003) β subunits of voltage-gated calcium channels. *J Bioenerg Biomembr* **35:**599–620.

Dourado MM and Dryer SE (1992) Changes in the electrical properties of chick ciliary ganglion neurones during embryonic development. *J Physiol* **449:**411–428.

Gola M and Crest M (1993) Colocalization of active K_{Ca} channels and Ca^{2+} channels within Ca^{2+} domains in helix neurons. *Neuron* **10:**689–699.

Gonzalez-Gutierrez G, Miranda-Laferte E, Neely A, and Hidalgo P (2007) The Src homology 3 domain of the β-subunit of voltage-gated calcium channels promotes endocytosis via dynamin interaction. *J Biol Chem* **282:**2156–2162.

Grunnet M and Kaufmann WA (2004) Coassembly of big conductance Ca^{2+}-activated K^+ channels and L-type voltage-gated Ca^{2+} channels in rat brain. *J Biol Chem* **279:**36445–36453.

Hidalgo P, Gonzalez-Gutierrez G, Garcia-Olivares J, and Neely A (2006) The $\alpha1$-β subunit interaction that modulates calcium channel activity is reversible and requires a competent α-interaction domain. *J Biol Chem* **281:**24104–24110.

Jiang Y, Pico A, Cadene M, Chait BT, and MacKinnon R (2001) Structure of the RCK domain from the *E. Coli* K^+ channel and demonstration of its presence in the human BK channel. *Neuron* **29:**593–601.

Kim EY, Ridgway LD, and Dryer SE (2007a) Interactions with filamin A stimulate surface expression of large conductance Ca^{2+}-activated K^+ channels in the absence of direct actin binding. *Mol Pharmacol* **72:**622–630.

Kim EY, Ridgway LD, Zou S, Chiu YH, and Dryer SE (2007b) Alternatively spliced C-terminal domains regulate the surface expression of large conductance calcium-activated potassium channels. *Neuroscience* **146:**1652–1661.

Kim EY, Zou S, Ridgway LD, and Dryer SE (2007c) β1-subunits increase surface expression of a large-conductance Ca^{2+}-activated K^+ channel isoform. *J Neurophysiol* **97:**3508–3516.

Lhuillier L and Dryer SE (1999) TGFβ1 regulates the gating properties of intermediate-conductance K_{Ca} channels in developing parasympathetic neurons. *J Neurophysiol* **82:**1627–1631.

Lhuillier L and Dryer SE (2002) Developmental regulation of neuronal K_{Ca} channels by TGFβ1: an essential role for PI3 kinase signaling and membrane insertion. *J Neurophysiol* **88:**954–964.

Loane DJ, Lima PA, and Marrion NV (2007) Co-assembly of N-type Ca^{2+} and BK channels underlies functional coupling in rat brain. *J Cell Sci* **120:**985–995.

Magleby KL (2003) Gating mechanism of BK (Slo1) channels: so near, yet so far. *J Gen Physiol* **121:**81–96.

Marrion NV and Tavalin SJ (1998) Selective activation of Ca^{2+}-activated K^+ channels by co-localized Ca^{2+} channels in hippocampal neurons. *Nature* **395:**900–905.

Prakriya M and Lingle CJ (2000) Activation of BK channels in rat chromaffin cells requires summation of Ca^{2+} influx from multiple Ca^{2+} channels. *J Neurophysiol* **84:**1123–1135.

Salkoff L, Butler A, Ferreira G, Santi C, and Wei A (2006) High-conductance potassium channels of the SLO family. *Nat Rev Neurosci* **7:**921–931.

Schreiber M and Salkoff L (1997) A novel calcium-sensing domain in the BK channel. *Biophys J* **73:**1355–1363.

Shipston MJ (2001) Alternative splicing of potassium channels: a dynamic switch of cellular excitability. *Trends Cell Biol* **11:**353–358.

Takahashi SX, Miriyala J, Tay LH, Yue DT, and Colecraft HM (2005) A CaVbeta SH3/guanylate kinase domain interaction regulates multiple properties of voltage-gated Ca^{2+} channels. *J Gen Physiol* **126:**365–377.

Thurm H, Fakler B, and Oliver D (2005) Ca^{2+}-independent activation of BK_{Ca} channels at negative potentials in mammalian inner hair cells. *J Physiol* **569:**137–151.

Tian L, Chen L, McClafferty H, Sailer CA, Ruth P, Knaus HG, and Shipston MJ (2006) A noncanonical SH3 domain binding motif links BK channels to the actin cytoskeleton via the SH3 adapter cortactin. *FASEB J* **20:**2588–2590.

Van Petegem F, Clark KA, Chatelain FC, and Minor DL Jr (2004) Structure of a complex between a voltage-gated calcium channel β-subunit and an α-subunit domain. *Nature* **429:**671–675.

Wisgirda ME and Dryer SE (1994) Functional dependence of Ca^{2+}-activated K^+ current on L- and N-type Ca^{2+} channels: differences between chicken sympathetic and parasympathetic neurons suggest different regulatory mechanisms. *Proc Natl Acad Sci U S A* **91:**2858–2862.

Xia XM, Zeng XH, and Lingle CJ (2002) Multiple regulatory sites in large-conductance calcium-activated potassium channels. *Nature* **418:**880–884.

Zeng XH, Xia XM, and Lingle CJ (2005) Divalent cation sensitivity of BK channel activation supports the existence of three distinct binding sites. *J Gen Physiol* **125:**273–286.

Zhang X, Solaro CR, and Lingle CJ (2001) Allosteric regulation of BK channel gating by Ca^{2+} and Mg^{2+} through a nonselective, low affinity divalent cation site. *J Gen Physiol* **118:**607–635.

Address correspondence to: Dr. Stuart E. Dryer, Department of Biology and Biochemistry, University of Houston, 4800 Calhoun, Houston, TX 77204-5001. E-mail: sdryer@uh.edu